

## Slip at the surface of a general axi-symmetric body rotating in a viscous fluid

E. A. ASHMAWY

*Department of Mathematics  
Faculty of Science  
Alexandria University  
Alexandria, Egypt  
e-mail: emad\_ashm@yahoo.com*

THE ROTATIONAL MOTION of an arbitrary axi-symmetric body in a viscous fluid is discussed using a combined analytical-numerical technique. A singularity method based on a continuous distribution of a set of Sampson spherical singularities, namely Sampsonlets, along the axis of symmetry within the body, is applied to find the general solution for the fluid velocity that satisfies the general slip boundary condition. Employing a constant and linear approximation for the density functions and applying the collocation technique to satisfy the slip boundary condition on the surface of the body, a system of linear algebraic equations is obtained to be solved numerically. The couple exerted on a prolate and oblate spheroid and on a prolate and oblate Cassini ovals is evaluated for various values of the aspect ratio  $a/b$  and for different values of the slip parameter, where  $a$  and  $b$  are the major and minor semi-axes of the particle respectively. The CPU time elapsed during numerical calculations is measured and tabulated. Numerical work shows that convergence to at least six decimal places is achieved.

**Key words:** viscous fluid, rotational motion, Sampsonlet singularities, axi-symmetric particle, Cassini ovals, collocation technique.

Copyright © 2011 by IPPT PAN

### 1. Introduction

THE COUPLE EXPERIENCED by axi-symmetrical bodies rotating steadily in an incompressible viscous fluid is of practical interest in many technological applications. It is required for designation and calibration of viscometers [1]. This prompted many authors to discuss the rotational motion of axially symmetric bodies in steady incompressible viscous fluid flows. JEFFERY [2] has used the curvilinear coordinates to solve the problem of slow steady rotation of spheroids in an infinite viscous fluid. An elegant formula for evaluating the couple experienced by an axially symmetric body rotating about its axis of revolution in an incompressible viscous fluid flow is obtained by KANWAL [1]. BRENNER [3] has used the symbolic operator method to obtain the hydrodynamic resistance of

a rigid particle of arbitrary shape, immersed in an arbitrary quasistatic Stokes flow extending to infinity.

In the literature, an increasing number of authors have treated Stokes flow problems using numerical methods. YU *et al.* [4] have discussed the rotation of a spheroid in a Couette flow numerically with the method of distributed Lagrangian multiplier based on fictitious domain. The boundary integral method has been utilized by many authors, e.g. [5]–[8]. One of the important numerical methods available for solving Stokes flow problems is the singularity method which is based on the choice of appropriate basic spherical singularities, namely Sampsonlet singularities, distributed discretely or continuously along the axis of symmetry of the body immersed in the fluid. Actually the singularity method has been known since the pioneering work of LORENTZ [9], OSEEN [10] and BURGERS [11]. Later, the singularity method has been developed and applied to a number of Stokes flows, e.g. [12–17]. KOHR and POP, in their book [18], discussed the implementation of the singularity method for Stokes flow past or due to the motion of a solid sphere above a plane wall. FENG and WU [19] investigated the electrophoretic motion of an arbitrary prolate body of revolution perpendicular to an infinite conducting planar wall using a combined analytical-numerical method. WAN and KEH [20] investigated the problem of the rotation of a prolate or oblate ellipsoidal particle about its axis of revolution in a viscous fluid using the singularity method.

The Navier–Stokes equations of fluid flow are typically solved under no-slip boundary conditions, i.e., assuming that the layer of liquid next to a solid surface moves with the local velocity of the surface. The no-slip condition was a characterized issue in the early development of fluid mechanics. Experimental observations appeared to confirm its validity over a vast array of differing situations. However, in the last century several studies have shown that this condition might not always hold, and that fluid slippage might occur at the solid boundary [21–24]. There exist situations in which the no-slip boundary condition leads to singular or unrealistic behavior; for example, the spreading of a liquid on a solid substrate [25–28], corner flow [29, 30] and extrusion of polymer melts from a capillary tube [31, 32]. O’NEILL *et al.* [33] used a linear slip, Basset-type [34], boundary condition to remove the contact-line singularity that would otherwise prevent the movement of a half-submerged sphere normal to a planar free surface bounding a semi-infinite viscous fluid. In fact, nearly two hundred years ago NAVIER [35] proposed a general boundary condition that permits the possibility of fluid slip at a solid boundary. This boundary condition assumes that the tangential velocity of the fluid relative to the solid at a point on its surface is proportional to the tangential stress acting at that point. The constant of proportionality between these two quantities may be termed as a coefficient of sliding friction, it is assumed to depend only on the

nature of the fluid and solid surface [35]. BASSET [34] derived expressions for the force and couple exerted by the fluid on a translating and rotating rigid sphere with a slip boundary condition at its surface (e.g., a settling aerosol sphere). Later, the quasisteady translation and steady rotation of a slip spherical particle in a slip spherical cavity are also theoretically studied in [36]. While the solutions of the Stokesian flow equations with slip conditions are of substantial interest for gases, recently it has been noted that slip conditions are of interest for liquids as well, particularly with respect to microscopic sense. BARRAT and BOCQUET [37] have used molecular dynamics to compute slip for liquids. PIT *et al.* [38] has measured slip for hexadecane on several modified sapphire surface using a rotating disk. NETO *et al.* [39] provide an excellent review of experimental studies regarding the phenomenon of slip of Newtonian fluids at solid interface. They give a particular attention to the factors that affect the fluid slippage at the solid boundary such as surface roughness, wet ability and the presence of gaseous layers might have on the measured interfacial slip. In recent years, there has been an increased interest in using the slip boundary condition for Newtonian fluids [40–46], and for micropolar and microstretch fluids [47–49].

The goal of the present work is to discuss the slow steady rotational motion of a general axi-symmetric slip particle in an incompressible viscous fluid, in the limit of small Reynolds number, about its axis of revolution. The general slip boundary condition is applied at the surface of the body. A singularity method based on a continuous distribution of a set of Sampsonlet singularities along the axis of symmetry of the body is used to obtain the solution of the problem at hand. The total couple acting on the surface of the body is calculated for various values of the slip parameter and the aspect ratio of the body. Numerical results are obtained for the special cases of prolate spheroid, prolate Cassini oval, oblate spheroid and oblate Cassini oval particles.

## 2. Mathematical formulation

The slow steady rotational motion of a general axi-symmetric slip particle in an incompressible viscous fluid along its axis of revolution is considered as shown in Fig. 1. It is convenient to use both the circular cylindrical coordinates  $(\rho, \phi, z)$  and the spherical coordinates  $(r, \theta, \phi)$ , with the center of the solid particle at the origin of the coordinates. Due to symmetry of the fluid flow and the solid particle, the fluid velocity vector has components  $(0, 0, q_\phi)$  in the spherical coordinate system. The relations between the two coordinate systems are:

$$(2.1) \quad r = \sqrt{\rho^2 + z^2}, \quad \theta = \cos^{-1} \left( \frac{z}{\sqrt{\rho^2 + z^2}} \right).$$

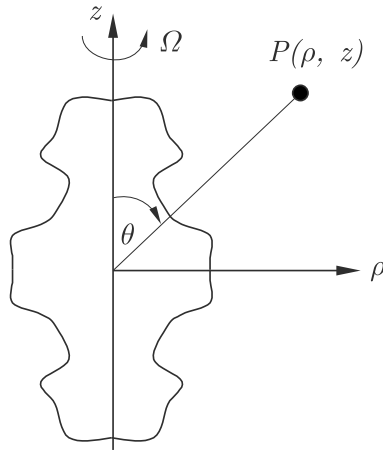


FIG. 1. Geometrical sketch for the solid particle  $S_p$ .

The velocity field of the fluid flow at low Reynolds number satisfies the differential equation

$$(2.2) \quad E^2(\rho q_\phi) = 0,$$

where

$$(2.3) \quad E^2 = \rho \frac{\partial}{\partial \rho} \left( \frac{1}{\rho} \frac{\partial}{\partial \rho} \right) + \frac{\partial^2}{\partial z^2}.$$

The slip boundary condition states that the relative tangential velocity of the fluid at the surface of the body is proportional to the local tangential stress. So, assuming that the solid particle rotates along positive  $z$ -direction with a constant angular speed  $\Omega$ , the slip boundary condition, in the cylindrical coordinate system, is taking the form

$$(2.4) \quad \beta(q_\phi - \rho\Omega) = n_\rho t_{\rho\phi} + n_z t_{z\phi} \quad \text{on } S_p,$$

where  $n_\rho$  and  $n_z$  are the local  $\rho$  and  $z$  components of the unit vector  $\mathbf{n}$  normal to the solid particle  $S_p$  and  $\beta$  ( $0 \leq \beta \leq 1$ ) is termed the slip parameter. Moreover, the fluid is at rest at infinity.

The general bounded solution for the differential equation (2.2) has the form

$$(2.5) \quad q_\phi(\rho, z) = \sum_{n=1}^{\infty} A_n A_{1n}(\rho, z).$$

Also, the shear stress components of the flow field are of the form

$$(2.6) \quad t_{\rho\phi}(\rho, z) = \sum_{n=1}^{\infty} A_n A_{2n}(\rho, z),$$

$$(2.7) \quad t_{z\phi}(\rho, z) = \sum_{n=1}^{\infty} A_n A_{3n}(\rho, z),$$

where  $A_n$  are unknown constants to be determined from the imposed boundary conditions, and the functions  $A_{kn}(\rho, z)$ ,  $k = 1, 2, 3$  are listed in the Appendix.

The total couple,  $C\mathbf{e}_\phi$ , exerted by the fluid on the surface of the solid particle  $S_p$  can be obtained using the following simple formula [1]:

$$(2.8) \quad C = 8\pi\mu \lim_{r \rightarrow \infty} \left( \frac{r^3 q_\phi}{\rho} \right),$$

where  $\mu$  is the fluid viscosity.

For the purpose of comparison, we note that the expression for the total couple acting on the surface of a slightly deformed colloidal sphere experiencing slip correct to the second order in the small parameter  $\varepsilon$  characterising the deformation, has been obtained by CHANG and KEH [50] as

$$(2.9) \quad C = 8\pi\mu b^3 \Omega \left\{ \frac{\beta b}{\beta b + 3\mu} - \varepsilon \frac{3\beta b(\beta b + \mu)}{5(\beta b + 3\mu)^2} + \varepsilon^2 \frac{3(\beta b)^4 \delta}{175(\beta b + 3\mu)^3(\beta b + 5\mu)} \right\},$$

where

$$\varepsilon = (1 - a/b) < 0, \quad \delta = \left\{ 1 + 3 \frac{\mu}{\beta b} + 36 \left( \frac{\mu}{\beta b} \right)^2 + 150 \left( \frac{\mu}{\beta b} \right)^3 \right\}.$$

### 3. Rotation of a general axi-symmetric prolate particle

In this section we consider the axi-symmetric fluid flow generated by the rotational motion of an arbitrary prolate spheroid or Cassini oval prolate particle. The particle rotates about its axis of revolution assuming slip boundary condition. A line segment  $AB$  is taken on the axis of revolution inside the particle, where the coordinates of the end points  $A$  and  $B$  are  $(\rho = 0, z = -c_1)$  and  $(\rho = 0, z = c_2)$ , respectively, in which  $c_1$  and  $c_2$  are positive constants. The general solution of the flow field outside the prolate particle can be constructed by a continuous distribution of a set of Sampsonlet singularities over the line segment  $AB$  [15–19]. Then, the Eqs. (2.5)–(2.7) can be represented as follows:

$$(3.1) \quad \begin{bmatrix} q_\phi \\ t_{\rho\phi} \\ t_{z\phi} \end{bmatrix} = \sum_{n=1}^{\infty} \int_{-c_1}^{c_2} \left\{ A_n(t) \begin{bmatrix} A_{1n}(\rho, z - t) \\ A_{2n}(\rho, z - t) \\ A_{3n}(\rho, z - t) \end{bmatrix} \right\} dt.$$

One can obtain the non-dimensional couple exerted by the fluid on the body from direct substitution of (2.5) into (2.8) to be

$$(3.2) \quad C^* = \frac{C}{8\pi\mu b^3\Omega} = \frac{1}{b^3\Omega} \int_{-c_1}^{c_2} A_1(t)dt.$$

The interval  $AB$  is divided into  $M$  segments; the length of each segment is the same. The density distribution functions on each segment are assumed to be constants. The coordinates of the two end points of the  $m$ -th segment are considered to be  $(0, t_{m-1})$  and  $(0, t_m)$ , where  $t_j = -c_1 + j(c_1 + c_2)/M$ ,  $j = 1, 2, \dots, M-1$  and  $t_0 = -c_1$ ,  $t_M = c_2$ . The density distribution functions in the  $m$ -th segment are given by the following linear relations:

$$(3.3) \quad A_n(t) = \frac{t - t_{m-1}}{t_m - t_{m-1}} A_{nm} + \frac{t_m - t}{t_m - t_{m-1}} A_{n(m-1)} \quad \text{for } t_{m-1} \leq t \leq t_m,$$

where  $A_{n(m-1)}$  and  $A_{nm}$  are the values of density distribution constants at the points  $t_{m-1}$  and  $t_m$ , respectively.

If the boundary  $S_p$  is approximated by satisfying condition (2.4) at  $N$  discrete points, thus the infinite series is truncated after  $N$  terms. Substituting relations (3.3) into (3.1), we get

$$(3.4) \quad \begin{bmatrix} q_\phi \\ t_{\rho\phi} \\ t_{z\phi} \end{bmatrix} = \sum_{n=1}^N \sum_{m=1}^M \left\{ \begin{bmatrix} U_{nm}^{(11)}(\rho, z) \\ U_{nm}^{(21)}(\rho, z) \\ U_{nm}^{(31)}(\rho, z) \end{bmatrix} A_{n(m-1)} + \begin{bmatrix} U_{nm}^{(12)}(\rho, z) \\ U_{nm}^{(22)}(\rho, z) \\ U_{nm}^{(32)}(\rho, z) \end{bmatrix} A_{nm} \right\},$$

where the functions  $U_{nm}^{(ij)}(\rho, z)$ ,  $i = 1, 2, 3$  and  $j = 1, 2$ , are given in the Appendix.

Substituting relations (3.4) into the boundary condition (2.4) we arrive at

$$(3.5) \quad \sum_{m=1}^M \sum_{n=1}^N \left\{ \left[ U_{nm}^{(11)}(\rho, z) - \frac{n_\rho}{\beta} U_{nm}^{(21)}(\rho, z) - \frac{n_z}{\beta} U_{nm}^{(31)}(\rho, z) \right] A_{n(m-1)} + \left[ U_{nm}^{(12)}(\rho, z) - \frac{n_\rho}{\beta} U_{nm}^{(22)}(\rho, z) - \frac{n_z}{\beta} U_{nm}^{(32)}(\rho, z) \right] A_{nm} \right\} = \rho\Omega \quad \text{on } S_p.$$

The collocation method approximates the boundary conditions on  $S_p$  by satisfying Eq. (3.5) at  $N(M+1)$  discrete values of  $z$  (rings) on its surface. This generates a set of  $N(M+1)$  simultaneous linear algebraic equations, which can be solved numerically to give the  $N(M+1)$  required density constants.

The non-dimensional couple can be evaluated from (3.2) to be

$$(3.6) \quad C^* = \frac{1}{2b^3\Omega} \sum_{m=1}^M (A_{1(m-1)} + A_{1m})(t_m - t_{m-1}).$$

The exact formula for the couple acting on a prolate spheroid, rotating with angular velocity  $\Omega$  about its axis of revolution in an unbounded viscous fluid flow assuming no-slip boundary conditions, is obtained by HAPPEL and BRENNER [21] as

$$(3.7) \quad C_s = 8\pi\mu b^3\Omega \left[ \frac{3}{2}\sqrt{\lambda^2 - 1}\{\lambda - (\lambda^2 - 1)\coth^{-1}(\lambda)\} \right]^{-1},$$

where

$$\lambda = \frac{a}{\sqrt{a^2 - b^2}}.$$

### 3.1. Rotation of a prolate spheroid particle

The above-mentioned method is employed to obtain the solution of the problem of the rotational motion of a prolate spheroid in a viscous fluid, which is otherwise at rest. WAN and KEH [20] have obtained the couple exerted on the surface of a spheroidal prolate particle correct to five decimal places with  $M = 60$ . Here, we have obtained the total couple acting on the surface of the spheroidal prolate particle correct to six decimal places, using  $N = 16$ , and evaluated the CPU time ( $T$  in seconds) elapsed in the numerical computations. All numerical results are performed on a Pentium 4 personal computer with processor of 3.0 GHz. The numerical integrations are performed using Romberg's integration formula with variable step. It is found that the results obtained are in a very good agreement with that of WAN and KEH [20].

In Table 1, numerical results of the non-dimensional couple,  $C^*$ , acting on the surface of the prolate spheroid, are listed for representative values of the aspect ratio  $a/b = 1.1, 1.5, 3.0, 5.0$  with various values of the slip parameter  $b\beta/\mu$ . Also the CPU time,  $T$  in seconds, elapsed in the numerical computations, is measured and presented. When the slip parameter  $b\beta/\mu \rightarrow \infty$ , we return to the classical case of no-slip boundary condition. The numerical results are compared with the approximate solutions given by (2.9) while for  $b\beta/\mu \rightarrow \infty$ , the results are compared with the exact solution given by (3.7). To achieve rapid convergence, the values of  $C^*$  are computed using the linear density distribution given by Eq. (3.3) at each sub-segment for different values of  $M$  with  $N = 16$ . As expected, the values of the couple increase monotonically with the increase of the slip parameter  $b\beta/\mu$ . Also, it can be observed that the increase of the aspect ratio  $a/b$  increases the total couple monotonically.

In Fig. 2, the non-dimensional couple  $C^*$  exerted by the fluid on the prolate spheroid is represented graphically against the non-dimensional slip parameter  $b\beta/\mu$  for various aspect ratios. It can be observed that the couple tends to be constant as the slip parameter  $b\beta/\mu$  exceeds a fixed value, namely 40.

**Table 1.** Numerical results for the non-dimensional couple acting on the surface of a spheroid prolate particle, for various values of its aspect ratio  $a/b$  and some values of the slip coefficient  $b\beta/\mu$  and the CPU time cost.

$b\beta/\mu$	$M$	$a/b = 1.1$		$a/b = 1.5$		$a/b = 3.0$		$a/b = 5.0$	
		$C^*$	$T$	$C^*$	$T$	$C^*$	$T$	$C^*$	$T$
0.1	2	0.034834	5.05	0.045381	7.68	0.050199	22.31	-3.443321	10.80
	3	0.034834	9.16	0.045381	12.51	0.086405	28.31	-0.035900	27.91
	4					0.086405	42.75	0.160016	43.93
	5							0.167201	57.25
	6							0.142358	70.05
	7							0.142131	89.00
	8							0.142145	102.63
	9							0.142145	107.35
	Approx	0.034835		0.045491		0.090388		0.162386	
1.0	2	0.268829	4.60	0.345338	15.75	0.415208	10.58	-5.157177	21.00
	3	0.268829	7.86	0.345338	19.35	0.639932	15.88	-0.598224	24.90
	4					0.639931	29.48	1.069979	31.30
	5					0.639931	36.96	1.047460	38.55
	6							1.039521	46.21
	7							1.039373	62.56
	8							1.039371	72.71
	9							1.039371	89.81
	Approx	0.268835		0.345871		0.658929		1.135714	
10.0	2	0.819027	5.96	1.019899	5.10	1.503489	7.86	-3.167952	17.80
	3	0.819027	10.76	1.019899	17.15	1.790063	11.95	-1.254604	22.46
	4					1.790047	17.28	2.668784	26.60
	5					1.790047	35.68	2.779308	35.08
	6							2.837533	54.80
	7							2.839079	68.73
	8							2.839079	62.31
	Approx.	0.819029		1.020105		1.800975		2.908043	
	$\infty$	2	1.060167	5.91	1.303749	15.50	2.201895	14.91	-7.571114
3		1.060167	19.93	1.303749	35.68	2.243937	32.68	-4.813517	36.68
4						2.243937	41.25	3.518275	53.18
5								3.530917	60.05
6								3.530283	63.91
7								3.530404	72.70
8								3.530404	78.80
Exact		1.060167		1.303749		2.243937		3.530404	

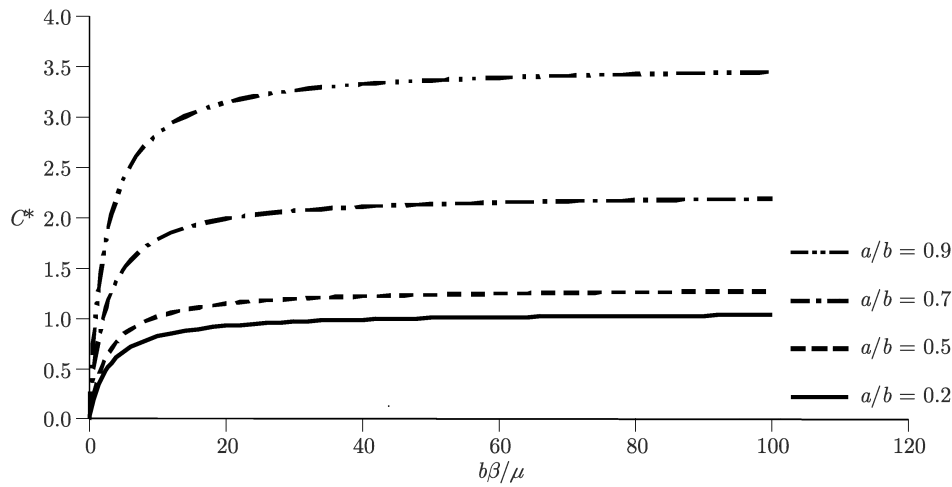


FIG. 2. Non-dimensional couple acting on the surface of a prolate spheroid.

### 3.2. Rotation of a Cassini oval prolate particle

Here, the presented method is applied to Cassini oval prolate particle of different shapes. When the parameter characterizing Cassini oval shape takes different values, the Cassini oval will have different forms, from convex contour to partial convex and partial concave contour. The surface of the Cassini oval prolate is represented by the polar equation

$$(3.8) \quad r^2 = \frac{1}{2} \left\{ (a^2 - b^2) \cos 2\theta + \sqrt{(a^2 + b^2)^2 - (a^2 - b^2)^2 \sin^2 2\theta} \right\},$$

where  $a$  and  $b$  are the semi-major and semi-minor axes of the Cassini oval.

In Figure 3, we illustrate geometrical sketches for the Cassini ovals for different values of the aspect ratio  $a/b$ .

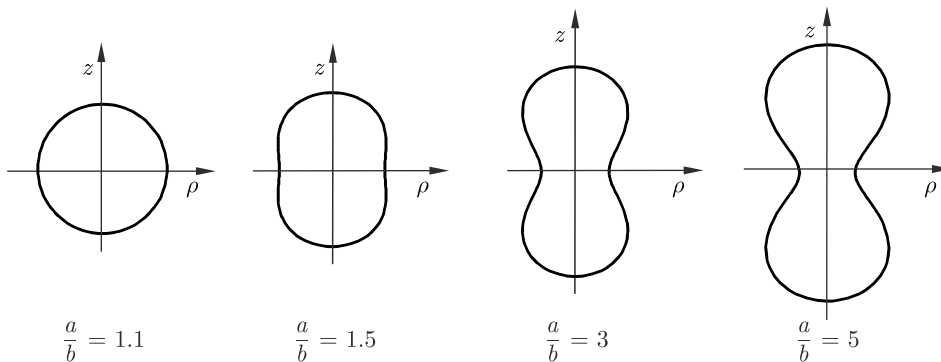


FIG. 3. Sketch for different prolate Cassini ovals.

The numerical solutions for the non-dimensional couple  $C^*$  of the axi-symmetric rotational motion of the prolate Cassini oval are listed in Table 2 for different values of the aspect ratio  $a/b = 1.1, 1.5, 3.0, 5.0$ . The CPU time elapsed in the numerical computations is also presented. The choices of the end points of the line segment for this case are somewhat indefinite. Here we have found that slightly different but reasonable choices of the end points of the line segment lead to almost the same solution for a given aspect ratio. The numerical results are compared with the approximate solutions given by (2.9).

**Table 2.** Numerical results for the non-dimensional couple acting on the surface of a Cassini oval prolate particle for various values of its aspect ratio  $a/b$  and some values of the slip coefficient  $b\beta/\mu$  and the CPU time cost.

$b\beta/\mu$	$M$	$a/b = 1.1$		$a/b = 1.5$		$a/b = 3.0$		$a/b = 5.0$	
		$C^*$	$T$	$C^*$	$T$	$C^*$	$T$	$C^*$	$T$
0.1	2	0.034985	1.33	0.049692	0.88	0.199570	1.16	0.950316	1.83
	3	0.034985	2.10	0.049692	2.18	0.199761	2.05	0.950619	2.16
	4					0.199761	3.28	0.950656	3.16
	5							0.950656	4.60
	Approx	0.034835		0.045491		0.090388		0.162386	
1.0	2	0.269931	1.00	0.376237	0.53	1.402014	1.73	5.980632	1.48
	3	0.269931	0.75	0.376237	1.05	1.403061	2.18	5.982143	1.33
	4					1.403061	2.26	5.982087	2.53
	5							5.982087	3.53
	Approx	0.268835		0.345871		0.658929		1.135714	
10.0	2	0.821927	1.15	1.099039	1.00	3.540820	1.41	12.726739	0.93
	3	0.821927	0.80	1.099039	1.46	3.541827	1.60	12.727736	1.78
	4					3.541827	3.25	12.727848	1.83
	5							12.727848	3.08
	Approx.	0.819029		1.020105		1.800975		2.908043	
$\infty$	2	1.063665	0.50	1.398664	1.00	4.269669	1.28	14.556165	1.03
	3	1.063665	0.91	1.398664	1.88	4.270179	1.65	14.556860	1.73
	4					4.270180	2.36	14.556866	2.45
	5					4.270180	3.41	14.556866	3.50
	Approx.	1.060167		1.303749		2.243937		3.530404	

In Figure 4, the non-dimensional couple  $C^*$  on the prolate Cassini oval is plotted against the slip parameter  $b\beta/\mu$  for several values of its aspect ratio. Similar to the results obtained for the motion of a prolate spheroid presented in the previous section, the values of  $C^*$  increases monotonically as the ratio  $a/b$  increases for fixed  $b\beta/\mu$ . Again,  $C^*$  increases monotonically as  $b\beta/\mu$  increases for a fixed aspect ratio. As the slip parameter  $b\beta/\mu$  exceeds a fixed value, namely 20,

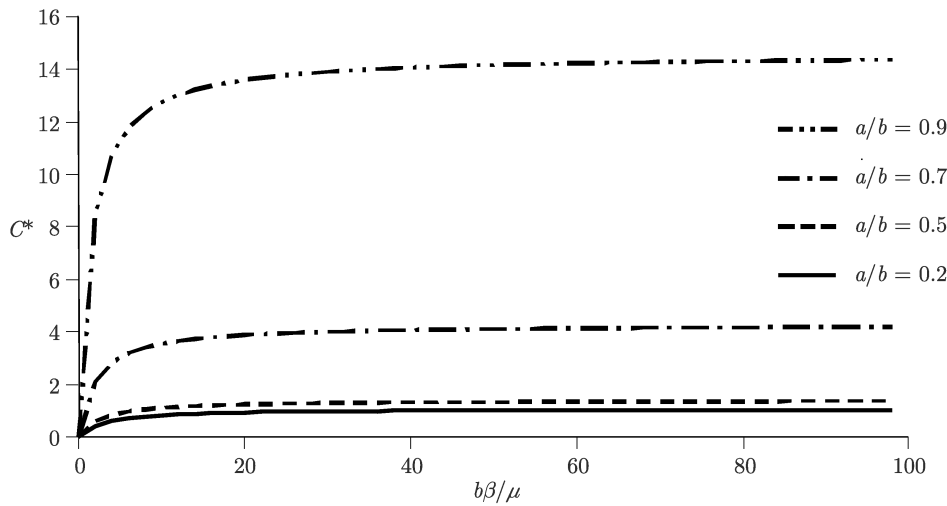


FIG. 4. Non-dimensional couple acting on the surface of a prolate Cassini ovals.

the couple tends to be constant. Also we observe that the values of the couple acting on Cassini ovals are greater than that on a prolate spheroid; this means that the couple depends strongly on dimensions and shape of the body.

#### 4. Rotation of a general axi-symmetric oblate particle

In this section, the method presented in the above sections is used to solve the Stokes' flow of an axi-symmetric oblate body, rotating about its axis of revolution in an incompressible viscous fluid. Here, the singularities should be distributed on the fundamental plane within the particle  $S_p$ . Since the particle and the fluid flow are axi-symmetric, then the fundamental plane should be a circular disk perpendicular to  $z$ -axis with its centre at the origin of the coordinates. Let  $Q(R, \psi, 0)$  to be an arbitrary point on  $S_p$ . Thus, the velocity at another point  $P(\rho, 0, z)$  generated by the spherical singularity at  $Q$  can be obtained in the form

$$(4.1) \quad \hat{q}_\phi(\rho, z) = \frac{(\rho - R \cos \psi)}{\rho^*} \sum_{n=1}^{\infty} B_n A_{1n}(\rho^*, z),$$

$$(4.2) \quad \hat{q}_\rho(\rho, z) = \frac{R \sin \psi}{\rho^*} \sum_{n=1}^{\infty} B_n A_{1n}(\rho^*, z),$$

where  $\rho^*$  is the distance from  $Q$  to the projection of  $P$  on the  $z$ -plane and is given by

$$(4.3) \quad \rho^* = \sqrt{\rho^2 + R^2 - 2\rho R \cos \psi}.$$

Since the motion is axi-symmetric, then the singularities must be distributed uniformly on the circles in  $S_p$  with their centers at the origin of coordinates. Hence, the unknown density distribution coefficients  $B_n$  appearing in Eqs. (4.1) and (4.2) are functions of  $R$  only. The total velocity of the flow field produced by the rotation of the oblate particle can be approximated by the superposition of the individual velocities in Eqs. (4.1) and (4.2), induced by the whole set of singularities on the fundamental disk  $S_p$ . Therefore, at an arbitrary point in the flow field, we have

$$(4.4) \quad q_\phi(\rho, z) = \sum_{n=1}^{\infty} \int_0^{2\pi} \int_0^d \frac{(\rho - R \cos \psi)}{\rho^*} B_n(R) A_{1n}(\rho^*, z) R dR d\psi,$$

where  $d$  is the radius of the fundamental disk  $S_p$ . The corresponding integral for  $\hat{q}_\rho$  becomes identically zero. The unknown density distribution functions  $B_n(R)$  must be determined from the boundary conditions (2.4) together with the collocation technique. Also, the non-vanishing stress components are given by

$$(4.5) \quad t_{\rho\phi}(\rho, z) = \sum_{n=1}^{\infty} \int_0^{2\pi} \int_0^d B_n(R) A_{2n}^*(\rho^*, z) R dR d\psi,$$

$$(4.6) \quad t_{z\phi}(\rho, z) = \sum_{n=1}^{\infty} \int_0^{2\pi} \int_0^d \frac{(\rho - R \cos \psi)}{\rho^*} B_n(R) A_{3n}(\rho^*, z) R dR d\psi,$$

where the functions  $A_{2n}^*(\rho, z)$  are listed in the Appendix.

Substituting from (4.4) into (2.8), we obtain the total couple acting on the surface of the axi-symmetric oblate particle in the non-dimensional form

$$(4.7) \quad C^* = \frac{C}{8\pi\mu b^3\Omega} = \frac{1}{b^3\Omega} \int_0^{2\pi} \int_0^d B_1(R) R dR d\psi.$$

This can be simplified to the form

$$(4.8) \quad C^* = \frac{2\pi}{b^3\Omega} \int_0^d B_1(R) R dR.$$

The radius of the fundamental disk  $S_p$  is divided into equal  $M$  segments. The inner and outer radii of the  $j$ -th segment are, respectively,  $R_{j-1}$  and  $R_j$ , where  $R_j = jd/M$ ,  $j = 0, 1, \dots, M$ . To satisfy the boundary conditions (2.4), we use the multipole collocation technique. In the constant density distribution,

the density functions  $B_n(R)$  in each segment are assumed to be constant and the infinite series can be truncated after  $N$  terms, from which we can represent Eqs. (4.4)–(4.6) in the form

$$(4.9) \quad \begin{bmatrix} q_\phi \\ t_{\rho\phi} \\ t_{z\phi} \end{bmatrix} = \sum_{n=1}^N \sum_{m=1}^M \left\{ B_{nm} \begin{bmatrix} B_{nm}^{(11)}(\rho, z) \\ B_{nm}^{(21)}(\rho, z) \\ B_{nm}^{(31)}(\rho, z) \end{bmatrix} \right\},$$

where the functions  $B_{nm}^{(i1)}(\rho, z)$ ,  $i = 1, 2, 3$ , are given in the Appendix and  $B_{nm}$  are unknown constants to be determined from the boundary conditions.

Thus, the relation (4.8) reduces to the form

$$(4.10) \quad C^* = \frac{\pi}{b^3 \Omega} \sum_{m=1}^M B_{1m} (R_m^2 - R_{m-1}^2).$$

Applying the boundary condition (2.4), we get

$$(4.11) \quad \sum_{m=1}^M \sum_{n=1}^N B_{nm} \left\{ B_{nm}^{(11)}(\rho, z) - \frac{n_\rho}{\beta} B_{nm}^{(21)}(\rho, z) - \frac{n_z}{\beta} B_{nm}^{(31)}(\rho, z) \right\} = \rho \Omega \quad \text{on } S_p.$$

Thus, the collocation technique can be applied to satisfy the Eq. (4.11) and to determine the  $MN$  density constants  $B_{nm}$  required for the fluid velocity field. Once these constants are determined, the resultant couple exerted on the particle can be obtained from Eq. (4.10).

The exact solution for the couple acting on an oblate spheroid rotating with angular velocity  $\Omega$  about its axis of revolution in an unbounded viscous fluid flow assuming no-slip boundary conditions, is obtained by HAPPEL and BRENNER [21] as

$$(4.12) \quad C_s = 8\pi\mu b^3 \Omega \left[ \frac{3}{2} \sqrt{\lambda^2 + 1} \{(\lambda^2 + 1) \cot^{-1}(\lambda) - \lambda\} \right]^{-1},$$

where

$$\lambda = \frac{a}{\sqrt{b^2 - a^2}}.$$

#### 4.1. Rotation of an oblate spheroid particle

Analogous to Sec. 3, we apply the above-mentioned technique to obtain the total couple exerted by the fluid on the surface of an oblate spheroid particle. Table 3 shows the resultant couple exerted on the surface of an oblate spheroid for different aspect ratios and some values of the dimensionless slip parameter.

The results obtained are correct to six decimal places and the CPU time is measured and tabulated. Similar results are obtained by WAN and KEH [20] correct to five decimal places. They have used the value of  $M = 60$ . Here, we have used the value of  $M = 16$  while for the aspect ratio  $a/b = 0.2$ , the value  $M = 32$  is used. All results obtained are correct to six decimal places. The numerical results are compared with the approximate solutions given by (2.9) while for  $b\beta/\mu \rightarrow \infty$ , the results are compared with the exact solution given by (4.12).

**Table 3. Numerical results for the dimensionless couple exerted on the surface of an oblate spheroid for different aspect ratios and different values of the slip parameter and the CPU time cost.**

$b\beta/\mu$	$N$	$a/b = 0.2$		$a/b = 0.5$		$a/b = 0.7$		$a/b = 0.9$	
		$C^*$	$T$	$C^*$	$T$	$C^*$	$T$	$C^*$	$T$
0.1	2	0.014185	51.03	0.020112	48.56	0.024775	23.05	0.029717	19.78
	3	0.014183	216.41	0.020112	196.41	0.024775	91.75	0.029717	55.48
	4	0.014183	426.43						
	Approx	0.012889		0.019892		0.024735		0.029716	
1.0	2	0.112846	37.92	0.159535	21.90	0.194717	5.75	0.231341	4.96
	3	0.112844	132.31	0.159534	81.18	0.194717	26.05	0.231341	15.13
	4	0.112844	286.34	0.159534	133.36				
	Approx	0.105429		0.158371		0.194513		0.231335	
10.0	2	0.380142	16.52	0.523348	9.66	0.621018	3.30	0.719623	3.03
	3	0.380141	96.23	0.523348	34.71	0.621018	10.06	0.719623	10.86
	4	0.380141	165.34						
	Approx.	0.377624		0.523064		0.620966		0.719621	
$\infty$	2	0.534366	10.95	0.705020	7.43	0.821690	3.45	0.940177	4.10
	3	0.534368	30.61	0.705020	12.95	0.821690	7.81	0.940177	9.91
	4	0.534368	112.76						
	Exact	0.534368		0.705020		0.821690		0.940177	

Figure 5 shows the variation of the total dimensionless couple acting on the surface of an oblate spheroid particle of different aspect ratios against the non-dimensional slip parameter  $b\beta/\mu$ . It can be observed that the values of the couple tend to be constants as the slip coefficient exceeds certain values, depending also on the value of the corresponding aspect ratio. Also we see that the value of the couple increases monotonically as the value of the aspect ratio increases.

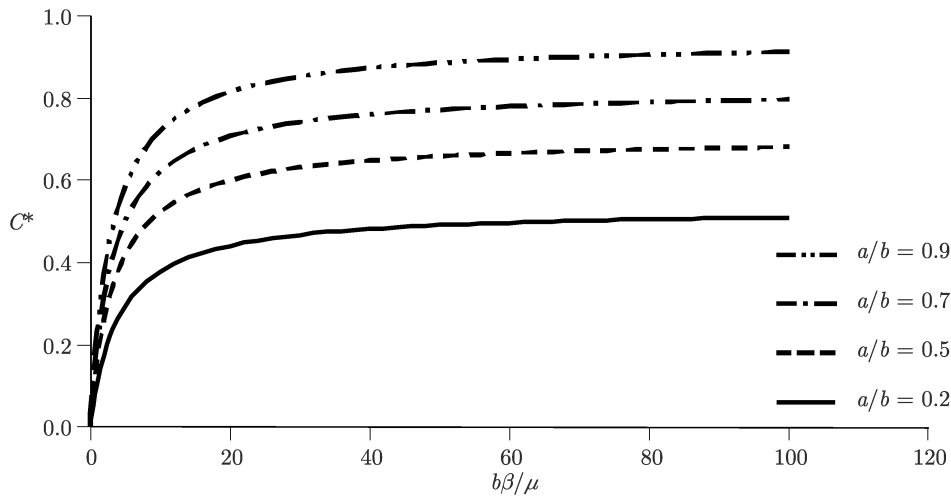


FIG. 5. Non-dimensional couple acting on the surface of an oblate spheroid particle.

#### 4.2. Rotation of an oblate Cassini oval

Here, we utilize the singularity method together with the collocation technique to obtain the total couple exerted by the fluid on the surface of an oblate Cassini oval of different shapes. The oblate Cassini oval will have different forms, from convex contour to partial convex and partial concave contour. The surface of the oblate Cassini oval is represented by the polar Eq. (3.8) with aspect ratio  $a/b < 1$ , as shown in Fig. 6.

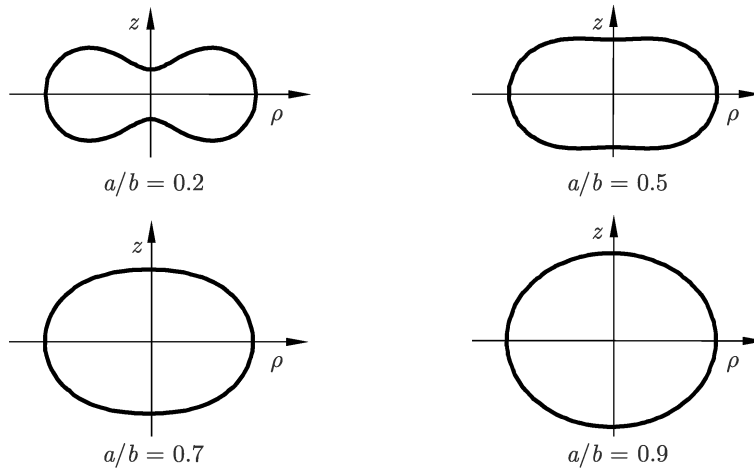


FIG. 6. Geometrical sketch for different oblate Cassini ovals.

In Table 4, we present the non-dimensional couple acting on the surface of an oblate Cassini oval for different values of the slip parameter  $b\beta/\mu$  and

the aspect ratio  $a/b$ . Also, the CPU time ( $T$  in seconds) elapsed in each iteration throughout the numerical computations is represented in Table 4. Here, we have taken  $M = 16$ . The results obtained are compared with the approximate solutions given by (2.9). It can be observed that for small aspect ratios, the approximate solution is poor while the numerical solution presented is more accurate. Also, comparing the results of Table 4 with that of Table 3 we conclude that the convergence achieved for Cassini ovals are much faster than that for spheroid.

**Table 4. Numerical results for the dimensionless couple exerted on the surface of an oblate Cassini oval for different aspect ratios and different values of the slip parameter and the CPU time cost.**

$b\beta/\mu$	$N$	$a/b = 0.2$		$a/b = 0.5$		$a/b = 0.7$		$a/b = 0.9$	
		$C^*$	$T$	$C^*$	$T$	$C^*$	$T$	$C^*$	$T$
0.1	2	0.020956	8.63	0.023194	22.10	0.025966	13.00	0.029858	18.91
	3	0.020955	45.75	0.023194	86.90	0.025966	56.63	0.029858	58.86
	4	0.020955	171.81						
	Approx.	0.012889		0.019892		0.024735		0.029716	
1.0	2	0.165443	3.41	0.182788	11.26	0.203592	15.23	0.232383	6.61
	3	0.165445	13.96	0.182780	74.21	0.203592	34.93	0.232383	22.55
	4	0.165445	72.25	0.182780	38.08				
	Approx.	0.105429		0.158371		0.194513		0.231335	
10.0	2	0.538931	6.91	0.588287	4.78	0.645167	4.98	0.722407	4.01
	3	0.538929	58.36	0.588287	16.51	0.645167	11.86	0.722407	19.45
	4	0.538929	110.00						
	Approx.	0.377624		0.523064		0.620966		0.719621	
$\infty$	2	0.724729	4.63	0.783029	4.08	0.850802	11.06	0.943538	4.45
	3	0.724730	22.75	0.783029	11.66	0.850802	22.00	0.943538	10.15
	4	0.724729	98.25						
	5	0.724729	105.25						
	Approx.	0.530971		0.704286		0.821543		0.940171	

Figure 7 shows the graphical representation of the dimensionless couple exerted by the fluid on the surface of an oblate Cassini oval of different aspect ratios against the dimensionless slip coefficient. As previous, it can be observed that the increase of the aspect ratio values increases the values of the total couple. The maximum value of the couple occurs when the particle becomes nearly a sphere.

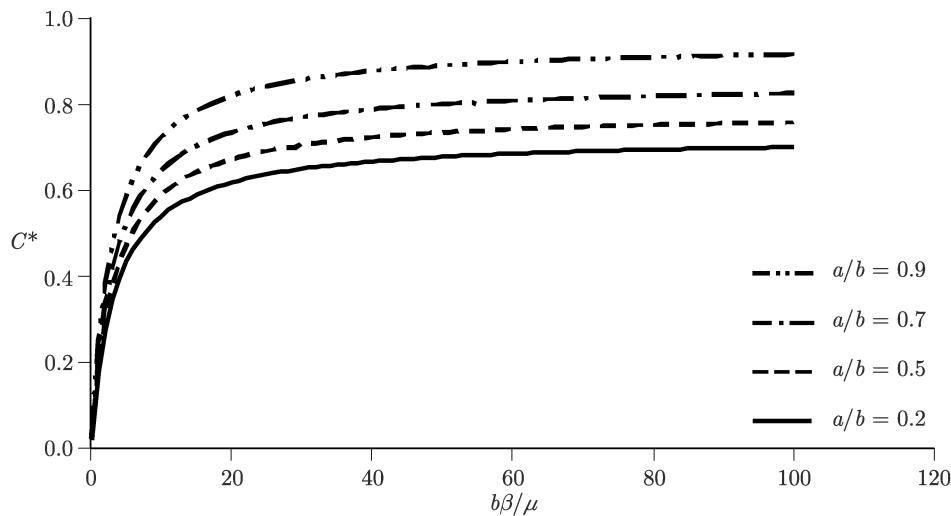


FIG. 7. Non-dimensional couple acting on the surface of an oblate Cassini oval.

## 5. Conclusion

In the present work, the slow steady rotational motion of a general axisymmetric body about its axis of symmetry with slip boundary condition has been investigated. The solution has been found by distributing a continuous set of Sampsonlets along the axis of symmetry of the prolate body and on the fundamental disk of the oblate body. The boundary collocation technique is then used. We have obtained numerical results for the couple exerted by the fluid on the body correct to six decimal places. We have also measured and tabulated the CPU time elapsed during numerical computations. For comparison, the exact solution for the rotation of a no-slip prolate and oblate spheroid about its axis of symmetry in an incompressible viscous fluid flow obtained by HAPPEL and BRENNER [21] is given by Eqs. (3.7) and (4.12), respectively. Also, the second-order approximate solutions for the axisymmetric rotation of a slip spheroid whose shape deviates slightly from that of a sphere obtained by CHANG and KEH [50], given by Eq. (2.9), are listed in the presented tables for comparison.

The results of the total couple exerted by the fluid on the body show that the method used converges rapidly, especially for Cassini ovals. Accurate solutions are obtained for the cases of spheroid prolate (or oblate) particle and Cassini oval prolate (or oblate) particle. It is observed that the couple experienced by a spheroid particle is smaller than that of Cassini ovals of the same aspect ratio. These results indicate that the value of the resultant couple acting on the solid particle depends greatly on dimensions and shape of the particle. Although the

analytical approximate solutions are somewhat accurate for prolate and oblate spheroids, it can be seen from the results listed in Table 2 and Table 4 that the approximate analytical solutions become poor for large aspect ratios of the prolate Cassini ovals and for small aspect ratios of the oblate Cassini ovals. To achieve convergence for the couple coefficient for values of aspect ratio greater than that listed in Table 1 and 2 or less than that in Table 3 and 4, large numbers of  $N$  and  $M$  are to be used. We note also that the convergence of the results obtained for the Cassini ovals are much faster than that of the spheroid particles. The solution of the problem of the rotational motion of axi-symmetric solid particle in a viscous fluid flow with no-slip boundary condition is simply recovered as a special case when the slip parameter  $b\beta/\mu$  tends to infinity, while the case of perfect slip can be also obtained when  $b\beta/\mu$  becomes zero.

## Appendix

$$(A.1) \quad A_{1n}(\rho, z) = (\rho^2 + z^2)^{-(n+1)/2} P_n^1(\zeta),$$

$$(A.2) \quad A_{2n}(\rho, z) = \mu\rho^{-1}(\rho^2 + z^2)^{-(n+1)/2} \\ \times \left[ \{(2n+1)\zeta^2 - (n+2)\}P_n^1(\zeta) - (n+1)\zeta P_{n-1}^1(\zeta) \right],$$

$$(A.3) \quad A_{3n}(\rho, z) = \mu(\rho^2 + z^2)^{-(n+2)/2} \left[ (n+1)P_{n-1}^1(\zeta) - (2n+1)\zeta P_n^1(\zeta) \right],$$

$$(A.4) \quad A_{2n}^*(\rho, z) = \mu \left[ \left\{ \frac{R^2 \sin^2 \psi}{\rho^{*3}} - \frac{(\rho - R \cos \psi)}{\rho \rho^*} \right\} A_{1n}(\rho^*, z) \right. \\ \left. + \frac{(\rho - R \cos \psi)^2}{\rho^{*3}} (\rho^{*2} + z^2)^{-(n+1)/2} \right. \\ \left. \times \left\{ (n+1)\zeta^* P_{n-1}^1(\zeta^*) + [(n+1) - (2n+1)\zeta^{*2}] P_n^1(\zeta^*) \right\} \right],$$

where  $\zeta = \cos \theta$  and  $P_n^1(\zeta)$  is the associated Legendre function.

$$(A.5) \quad U_{nm}^{(ik)} = \frac{(-1)^{k-1}}{t_m - t_{m-1}} \left\{ \delta_{1k} t_m A_{nm}^{(i1)} + \delta_{2k} t_{m-1} A_{nm}^{(i1)} - A_{nm}^{(i2)} \right\},$$

$$(A.6) \quad A_{nm}^{(i2)} = \int_{t_{m-1}}^{t_m} A_{in}(\rho, z-t)t dt, \quad i = 1, 2, 3,$$

where  $i = 1, 2, 3$ ,  $k = 1, 2$  and  $\delta_{ij}$  is the Kronecker delta.

$$(A.7) \quad B_{nm}^{(11)} = \int_0^{2\pi} \int_{R_{m-1}}^{R_m} \frac{(\rho - R \cos \psi)}{\rho^*} A_{1n}(\rho^*, z) R dR d\psi,$$

$$(A.8) \quad B_{nm}^{(21)} = \int_0^{2\pi} \int_{R_{m-1}}^{R_m} A_{2n}^*(\rho^*, z) R dR d\psi,$$

$$(A.9) \quad B_{nm}^{(31)} = \int_0^{2\pi} \int_{R_{m-1}}^{R_m} \frac{(\rho - R \cos \psi)}{\rho^*} A_{3n}(\rho^*, z) R dR d\psi.$$

## References

1. R.P. KANWAL, *Slow steady rotation of axially symmetric bodies in a viscous fluid*, J. Fluid Mech., **10**, 17–24, 1960.
2. G.B. JEFFREY, *On the steady rotation of a solid of revolution in a viscous fluid*, Proc. Lond. Math. Soc., **14**, 327–338, 1915.
3. H. BRENNER, *The Stokes resistance of an arbitrary particle – Part V. Symbolic operator representation of intrinsic resistance*, Chem. Eng. Sci., **21**, 97–109, 1966.
4. Z. YU, N. PHAN-THIEN, R.I. TANNER, *Rotation of a spheroid in a Couette flow at moderate Reynolds numbers*, Phys. Rev. E, **76**, 026310–026321, 2007.
5. G.K. YOUNGREN, A. ACRIVOS, *Stokes flow past a particle of arbitrary shape: a numerical method of solution*, J. Fluid Mech., **69**, 577–403, 1975.
6. S. WEINBAUM, P. GANATOS, Z. YAN, *Numerical multipole and boundary integral equation techniques in Stokes flow*, Ann. Rev. Fluid Mech. **22**, 275–316, 1990.
7. C. POZRIKIDIS, *Boundary integral and singularity methods for linearized viscous flow*, Cambridge University Press, Cambridge 1992.
8. M. KOHR, *Boundary integral method for Stokes flow past a solid sphere and a viscous drop*, Comput. Methods Appl. Mech. Engng., **190**, 5529–5542, 2001.
9. H.A. LORENTZ, *A general theorem concerning the motion of a viscous fluid and a few consequences derived from it*, Versl. Kon. Acad. Wet. Amst. **5**, 168–175, 1897.
10. C.W. OSEEN, *Neuere Methoden und Ergebnisse in der Hydrodynamik*, Leipzig, Akad. Verlagsgesellschaft M.B.H., 1927.
11. J.M. BURGERS, *On the motion of small particles of elongated form suspended in a viscous liquid: Chap. III of Second Report on Viscosity and Plasticity*, Kon. Ned. Akad. Wet. Verhand, **16**, 113–184, 1938.
12. Z. YAN, Y. ZHAO, W. LIU, *The Stokes flow induced by the rotation of a prolate axisymmetric body in the presence of an infinite planar boundary*, [in:] H. NIKI, M. KAWAHARA [Eds.], Computational Methods in Flow Analysis, **1**, Okayama University of Science, Okayama, Japan, 243–248, 1988.
13. J.R. BLAKE, A.T. CHWANG, *Fundamental singularities of viscous flow. Part I. The image system in the vicinity of stationary no-slip boundary*, J. Engng Math., **8**, 23–29, 1974.
14. P. GANATOS, S. WEINBAUM, R. PFEFFER, *Strong interaction theory for the creeping motion of a sphere between plan boundaries. Part 1. Perpendicular motion*, J. Fluid Mech. **99**, 739–753, 1980.

15. W. WANGI, *A new approach of treating the Stokes flow of nonslender prolate arbitrary axi-symmetrical body*, Sci. Sin. Ser. A, **27**, 731–744, 1984.
16. H.J. KEH, C.H. TSENG, *Slow motion of an arbitrary axisymmetric body along its axis of revolution and normal to a plane surface*, Int. J. Multiphase Flow, **20**, 185–210, 1994.
17. H.J. KEH, C.H. HUANG, *Slow motion of axi-symmetric slip particles along their axes of revolution*, Int. J. Engng. Sci., **42**, 1621–1644, 2004.
18. M. KOHR, I. POP, *Viscous Incompressible Flow for Low Reynolds Numbers*, WIT Press, Boston 2004.
19. J.-J. FENG, W.-Y. WU, *Electrophoretic motion of an arbitrary prolate body of revolution toward an infinite conducting wall*, J. Fluid Mech. **264**, 41–58, 1994.
20. Y.W. WAN, H.J. KEH, *Slow rotation of an axisymmetric slip particle about its axis of revolution*, CMES, **53**, 73–93, 2009.
21. J. HAPPEL, H. BRENNER, *Low Reynolds Number Hydrodynamics*, Noordhoff International Publishing, Leyden, Netherlands, 1973.
22. E.H. KENNARD, *Kinetic Theory of Gases*, McGraw-Hill, New York 1938.
23. D.K. HUTCHINS, M.H. HARPER, R.L. FELDER, *Slip correction measurements for solid spherical particles by modulated dynamic light scattering*, Aerosol. Sci. Technol., **22**, 202–218, 1995.
24. P.A. THOMPSON, S.M. TROIAN, *A general boundary condition for liquid flow at solid surfaces*, Nature (London), **389**, 360–362, 1997.
25. E.B. DUSSAN, *On the spreading of liquids on solid surfaces: static and dynamic contact lines*, Ann. Rev. Fluid. Mech., **11**, 371–400, 1979.
26. J. KOPLIK, J.R. BANAVAR, J.F. WILLEMSSEN, *Molecular dynamics of Poiseuille flow and moving contact lines*, Phys. Rev. Lett., **60**, 1282–1285, 1988.
27. P.A. THOMPSON, M.O. ROBBINS, *Simulations of contact line motion: slip and the dynamic contact angle*, Phys. Rev. Lett., **63**, 766–769, 1989.
28. P.A. THOMPSON, W.B. BRINKERHOFF, M.O. ROBBINS, *Microscopic studies of static and dynamic contact angles*, J. Adhesion Sci. Technol. **7**, 535–554, 1993.
29. H.K. MOFFATT, *Viscous and resistive eddies near a sharp corner*, J. Fluid Mech., **18**, 1–18, 1964.
30. J. KOPLIK, J.R. BANAVAR, *Corner flow in the sliding plate problem*, Phys. Fluids **7**, 3118–3125, 1995.
31. J.R.A. PEARSON, C.J.S. PETRIE, *Polymer Systems, Deformation and Flow*, R.E. WETTON, R.W. WHORLOW [Eds.], Macmillan, London, 163–187, 1968.
32. S. RICHARDSON, *On the no-slip boundary condition*, J. Fluid Mech., **59**, 707–719, 1973.
33. M.E. O’NEILL, K.B. RANGER, H. BRENNER, *Slip at the surface of a translating-rotating sphere bisected by a free surface bounding a semi-infinite viscous fluid: removal of the contact-line singularity*, Phys. Fluids, **29**, 913–924, 1986.
34. A.B. BASSET, *A Treatise on Hydrodynamics*, **2**, Dover, New York 1961.
35. C.L.M.H. NAVIER, *Memoirs de l’Academie*, Royale des Sciences de l’Institut de France, **1**, 414–416, 1823.

36. H.J. KEH, J.H. CHANG, *Boundary effects on the creeping-flow and thermophoretic motions of an aerosol particle in a spherical cavity*, Chem. Eng. Sci., **53**, 2365–2377, 1998.
37. J. BARRAT, L. BOCQUET, *Large slip effect at a nonwetting fluid-solid interface*, Phys. Rev. Lett., **82**, 4671–4674, 1999.
38. R. PIT, H. HERVET, L. LÉGER, *Direct Experimental Evidence of Slip in Hexadecane, Solid Interfaces*, Phys. Rev. Lett. **85**, 980–983, 2000.
39. C. NETO, D.R. EVANS, E. BONACCURSO, H.J. BUTT, V.S.J. CRAIG, *Boundary slip in Newtonian liquids, a review of experimental studies*, Rep. Progr. Phys., **68**, 2859–2897, 2005.
40. D.C. TRETHERWAY, C.D. MEINHART, *Apparent fluid slip at hydrophobic microchannel walls*, Phys. Fluids, **14**, L9–L12, 2002.
41. G. WILLMOTT, *Dynamics of a sphere with inhomogeneous slip boundary conditions in Stokes flow*, Phys. Rev., E **77**, 055302–055305, 2008.
42. H. SUN, C. LIU, *The slip boundary condition in the dynamics of solid particles immersed in Stokesian flows*, Solid State Commun., **150**, 990–1002, 2010.
43. H. ZHANG, Z. ZHANG, Y. ZHENG, H. YE, *Corrected second-order slip boundary condition for fluid flows in nanochannels*, Phys. Rev., E **81**, 066303–066308, 2010.
44. F. YANG, *Slip boundary condition for viscous flow over solid surfaces*, Chem. Eng. Comm., **197**, 544–550, 2010.
45. J.K. WHITMER, E. LUIJTEN, *Fluid-solid boundary conditions for multiparticle collision dynamics*, J. Phys. Condens. Matter, **22**, 104–106, 2010.
46. H. RAMKISSOON, *Slip flow past an approximate spheroid*, Acta Mech., **123**, 227–233, 1997.
47. H.H. SHERIEF, M.S. FALTAS, E.I. SAAD, *Slip at the surface of a sphere translating perpendicular to a plane wall in micropolar fluid*, Z. Angew. Math. Phys., **59**, 293–312, 2008.
48. Y.Y. LOK, I. POP, D.B. INGHAM, *Oblique stagnation slip flow of a micropolar fluid*, Meccanica, **45**, 187–198, 2010.
49. H.H. SHERIEF, M.S. FALTAS, E.A. ASHMAWY, *Galerkin representations and fundamental solutions for an axisymmetric microstretch fluid flow*, J. Fluid Mech., **619**, 277–293, 2009.
50. Y.C. CHANG, H.J. KEH, *Translation and rotation of slightly deformed colloidal spheres experiencing slip*, J. Colloid Interface Sci., **330**, 201–210, 2009.

Received April 1, 2010; revised version March 28, 2011.

---